Modern Physics Letters B
Vol. 28, No. 28 (2014) 1450224 (10 pages)

DOI: 10.1142/S0217984914502248

The effects of different polymerization agents on structural and optical properties of $(K_{0.5}Na_{0.5})NbO_3$ nanopowders synthesized by a facile green route

Gh. H. Khorrami*,‡, A. Kompany* and A. Khorsand Zak†

*Materials and Electroceramic Lab., Department of Physics, Ferdowsi University of Mashhad, Mashhad, Iran
†Nanotechnology Lab., Esfarayen University, Esfarayen, North Khorasan, Iran
‡khorrami1983@gmail.com

Received 12 July 2014
Accepted 14 October 2014
Published 12 November 2014

$(K_{0.5}N_{0.5})NbO_3$ lead-free nanopowders were synthesized by a modified sol–gel method in different media: gelatin, starch and chitosan, as polymerization and stabilizer agents. The proper temperature needed for calcinating the prepared gel was obtained using thermogravometric analysis (TGA). Structural and optical properties of the prepared powders were investigated and compared using X-ray diffraction (XRD), transmission electron microscopy (TEM) and UV-Vis diffused reflectance spectroscopy. The XRD patterns of the synthesized samples confirmed the formation of the orthorhombic structure at 600°C calcination temperature with no remarkable extra peaks. TEM images showed that the morphologies of the particles prepared in the three different media are cubic with the average size of about 69, 34 and 49 nm for gelatin, starch and chitosan, respectively. The value of the energy band gap of the samples was calculated by diffused reflectance spectroscopy, using Kubelka–Munk method. Our results showed that the type of the polymerization agent is important in preparing KNN nanoparticles and affects the structural and optical properties of the synthesized samples.

Keywords: KNN nanopowders; gelatin; starch; chitosan; structural properties; optical properties; Kubelka–Munk method.

1. Introduction

Piezoelectric materials such as lead zirconate titanate (PZT) and the related compounds are well known and important materials due to their excellent mechanical and electrical properties which play major roles in fabricating numerous devices such as transducers, transformers, sensors and actuators.[1–3] In recent years, because of the environmental concerns about the highly toxic nature of lead-based

‡Corresponding author.

ceramics including PZTs, lead free piezoelectric materials have attracted great attentions to replace PZTs. Among lead free piezoelectrics, alkaline niobates with perovskite structure are known to be good candidates to substitute the piezoelectric materials based on lead. This attention is due to their rather good piezoelectric, ferroelectric and electromechanical properties as well as having good electro-optical, nonlinear optical and photocatalytic properties.[2,4–7] Potassium sodium niobate $(K_xNa_{1-x})NbO_3$ (KNN) show good electrical properties specially at the morphotropic phase boundary (MPB) ($x = 0.5$).[8] The common method used for the synthesis of KNN powders is the solid state reaction, but it is difficult to obtain dense KNN compounds using this conventional method, because of the volatility of sodium and potassium oxides at high temperatures.[9] In comparison with solid state reaction, wet chemical methods based on hydrothermal,[10–12] solvothermal[13,14] and sol–gel[15–17] have the potential to produce powders with smaller particle size and better chemical uniformity at lower calcination temperatures. Also, preparation of nanoscale oxides by thermolysis method with inorganic–organic precursors has been reported in which the size of the particles can be controlled using a suitable precursor. Wohlrab *et al.* used Sugar-PVA matrix and activated carbon for the synthesis of alkali niobates.[18] Young *et al.* used ethylene diamine tetraacetic acid (EDTA) to synthesize KNN powders with the particle size in the range of 200–300 nm at 850°C calcination temperature.[16]

In this paper, we report a facile "green" synthesis of KNN nanoparticles using natural polymers (gelatin, starch and chitosan) as polymerization and stabilizer agents. The structural and optical properties of the samples synthesized in three different media are investigated and compared.

2. Experimental

2.1. *Materials and methods*

Potassium nitrate (KNO_3, $\geq 99\%$ purity, Sigma-Aldrich), sodium nitrate ($NaNO_3$, $\geq 99\%$ purity, Sigma-Aldrich) and ammonium niobate (V) oxalate hydrate ($C_4H_4NNbO_9 \cdot xH_2O$, 99.99% purity, Sigma-Aldrich) were used as the starting materials. Gelatin type B from bovine skin (Sigma-Aldrich), starch ($C_{12}H_{22}O_{11}$, Aldrich, ACS reagent) and chitosan (low molecular weight, Sigma-Aldrich) were used as the polymerization and stabilizer agents and distilled water, acetic acid and oleic acid as the solvents. In order to prepare 5 g of the final product 25 g of gelatin, starch and chitosan were dissolved in a proper solvent, separately. Gelatin and starch were dissolved in distilled water and chitosan in dilute aqueous acid from oleic and citric acids. Appropriate amounts of sodium and potassium nitrates and ammonium niobate (V) oxalate hydrate were dissolved in minimum amount of distilled water. Then these three solutions were added gradually to the first prepared solutions. The temperature of the oil bath was kept at 70°C while stirring until the gels were obtained. Finally, by drying the gels inside an oven at 80°C and then calcined at 600°C for 4 h the white KNN powders were produced. For

simplicity, KNN powders synthesized in gelatin, starch and chitosan media are shown by KNN-G, KNN-S and KNN-Ch, respectively.

2.2. *Characterizations*

In order to find out the optimum calcination temperature, the dried gel was analyzed by thermogravometric analyzer (DTG-60/60, Shimadzu). X-ray diffraction technique (XRD, Philips, X'pert, Cu-Kα) was used to study the lattice structure of the prepared powders. The morphology of the KNN powders was examined using transmission electron microscopy (TEM, CM120, Philips). UV-Vis diffused reflectance spectroscopy (Jasco, V-670) was applied to investigate the optical properties and to determine the value of the energy band gap of the prepared samples.

3. Results and Discussion

3.1. *Thermal analysis (TGA)*

Figure 1 shows the results of TGA of KNN-G, KNN-S and KNN-Ch dried gels and the corresponding derivatives in the range of room temperature to 800°C. The TGA curve of each sample decreases until about 500°C with mass loss of 72%, 84% and 81% for KNN-G, KNN-S and KNN-Ch, respectively. Three main mass loss regions are observed in the TGA curves. The first two regions are attributed to the decomposition of the polymer chains. The carboxylic compounds are decomposed and the pyrochlore phase is formed at temperatures less than 400. The third region of about 400–500°C, which is the main part of the curve, is due to the formation of the perovskite structure with a maximum mass loss rates at 477°C, 496°C and 510°C for KNN-G, KNN-S and KNN-Ch, respectively. It is also observed from the TGA curves that the appropriate calcination temperature is about 600°C for all the three samples.

3.2. *Structural analysis*

X-ray diffraction analysis was carried out in the range of $2\theta = 10$–$80°$. The XRD patterns of the synthesized KNN-G, KNN-S and KNN-Ch powders are shown in Fig. 2. The crystal structure of all the three samples is found to be orthorhombic as indexed (JCPDS, 32-0822). No other remarkable diffraction peaks, related to the impurities or pyrocholor phases, are detected.

The lattice parameters of the three prepared samples were calculated using least squares refinement method, which are presented in Table 1.

Figure 3 shows an image of the main diffraction peaks of KNN-G, KNN-S and KNN-Ch nanoparticles, which occur between 30.5° and 33.5°. The main peak intensity of KNN-G is higher comparing to KNN-S and KNN-Ch, showing better crystallinity of the KNN-G sample.

The average crystallite size of the samples were estimated by Scherrer equation ($D = k\lambda/(\beta_{hkl}\cos\theta)$) using the main diffraction peaks of the XRD patterns. In

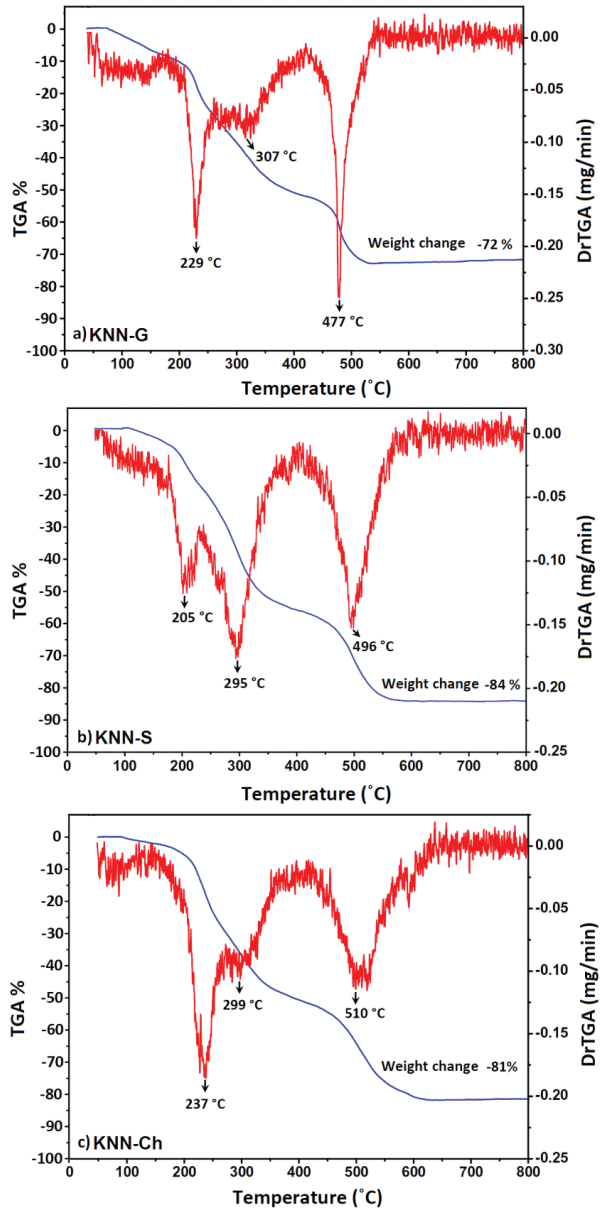

Fig. 1. (Color online) TGA curves of KNN gel in (a) chitosan, (b) starch, (c) gelatin media.

this formula, β_{hkl} is the full width half maximum (FWHM) of (hkl) diffraction peak, k is constant about unity and θ is the diffraction peak angle. It has been shown that the presence of lattice strain affects the position and broadening of the peaks in the XRD patterns.[19] So, it is more precise to consider the lattice strain

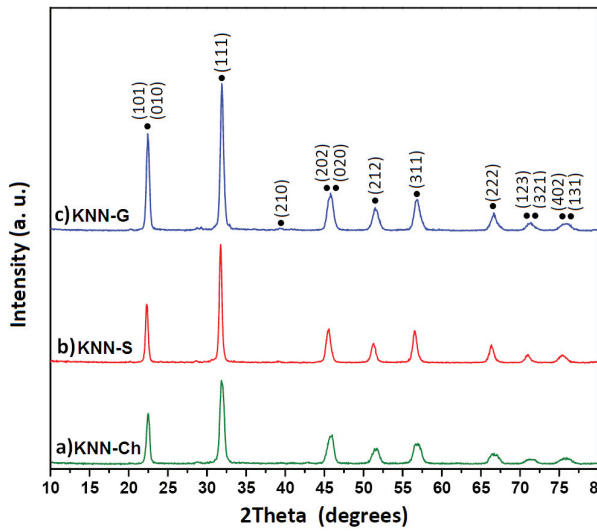

Fig. 2. (Color online) XRD patterns of KNN calcined at 600°C in (a) chitosan, (b) starch, (c) gelatin media.

Table 1. Lattice parameters of KNN-NPs prepared at different media.

Materials	$2\theta \pm 0.05$	d_{hkl} (Å)	hkl	Structure	Lattice parameter (Å)	V (Å^3)
KNN-Ch	22.51	3.94(8)	101	orthorhombic	$a = 5.572(2)$	124.41(3)
	31.96	2.79(9)	111		$b = 3.965(1)$	
					$c = 5.631(1)$	
KNN-G	22.49	3.95(2)	101	orthorhombic	$a = 5.576(9)$	124.12(1)
	31.95	2.80(0)	111		$b = 3.964(8)$	
					$c = 5.613(5)$	
KNN-S	22.35	3.97(6)	101	orthorhombic	$a = 5.636(3)$	126.33(2)
	31.78	2.81(4)	111		$b = 3.980(1)$	
					$c = 5.631(6)$	

for calculating the crystallite size. Size strain plot (SSP) method is the one which makes it possible to consider more diffraction peaks from XRD pattern to evaluate both the crystallite size and the lattice strain. Accordingly, we have

$$(d_{hkl}\beta_{hkl}\cos\theta)^2 = \frac{K}{D}(d_{hkl}^2\beta_{hkl}\cos\theta) + \left(\frac{\varepsilon}{2}\right)^2, \tag{1}$$

where K is a constant which depends on the shape of the particles and is 4/3. To estimate the crystallite size and the lattice strain, the term $(d\beta\cos\theta)^2$ was plotted against $d^2\beta\cos\theta$, as shown in Fig. 4. The obtained points are linearly fitted and the crystallite size is calculated from the slope of linearly fitted data and the lattice strain from y-intercept. The obtained crystallite size and the lattice strain of the KNN-G, KNN-S, and KNN-Ch samples are presented in Table 2.

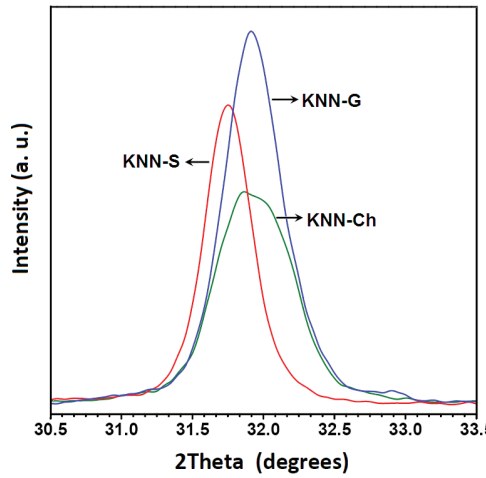

Fig. 3. (Color online) Main diffraction peaks of KNN calcined at 600°C in three different media.

Table 2. The crystallite size and lattice strain of the synthesized samples.

	Scherrer formula	Size strain plot	
Materials	Crystallite size (D) (nm)	Crystallite size (D) (nm)	Strain (ε) $\times 10^{-2}$
KNN-Ch	14.30(9)	19.90(1)	4.60(4)
KNN-G	19.79(5)	19.04(7)	3.52(1)
KNN-S	23.78(5)	19.07(4)	3.36(6)

3.3. *Morphology studies*

The TEM images and the corresponding size distribution histograms are presented in Fig. 5. The TEM images show that the KNN-G, KNN-S and KNN-Ch nanoparticles have grown in cubic shape. The average sizes of the prepared nanoparticles are about 69, 34 and 49 nm for KNN-G, KNN-S and KNN-Ch, respectively. KNN-S nanoparticles are smaller than KNN-S and KNN-Ch nanoparticles. However, the distribution of KNN nanoparticles prepared in gelatin medium (KNN-G) is more homogenous in comparison with KNN-S and KNN-Ch nanoparticles.

3.4. *Optical analysis*

Study of the optical properties of the prepared samples was carried out based on diffused reflectance spectroscopy, which is a more convenient technique to characterize unsupported nanoparticles, comparing to UV-Vis absorption spectroscopy, since this method takes the advantage of scattering phenomenon for powder materials.[21] The reflectance and the corresponding absorbance of the synthesized KNN-G, KNN-S and KNN-Ch samples were measured in the wavelength range 200 nm to 800 nm (Fig. 6).

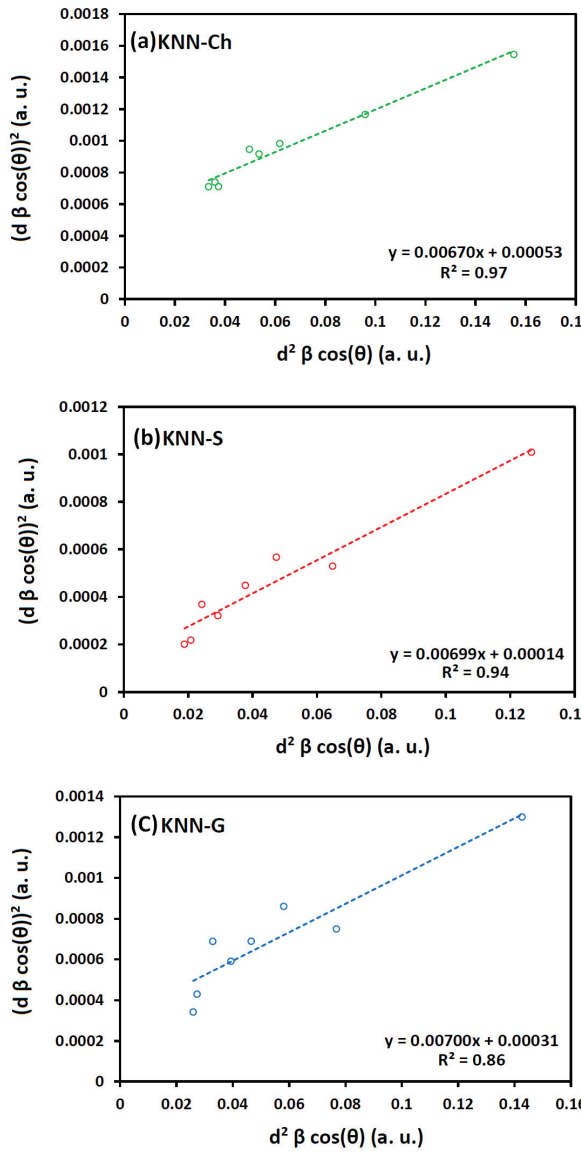

Fig. 4. (Color online) SSP plots of KNN calcined at 600°C in (a) chitosan, (b) starch, (c) gelatin media.

It is observed that the absorption edge of KNN-Ch occurs at higher wavelength compared to KNN-G and KNN-S. The optical band gap of the specimens can be calculated by Kubelka–Munk method using Tauc relation:[22]

$$(\alpha h\nu)^{\frac{1}{m}} = c(hv - E_g) \tag{2}$$

where m is chosen 2 for indirect and $\frac{1}{2}$ for direct band gaps, respectively. $(\alpha h\nu)^{\frac{1}{m}}$

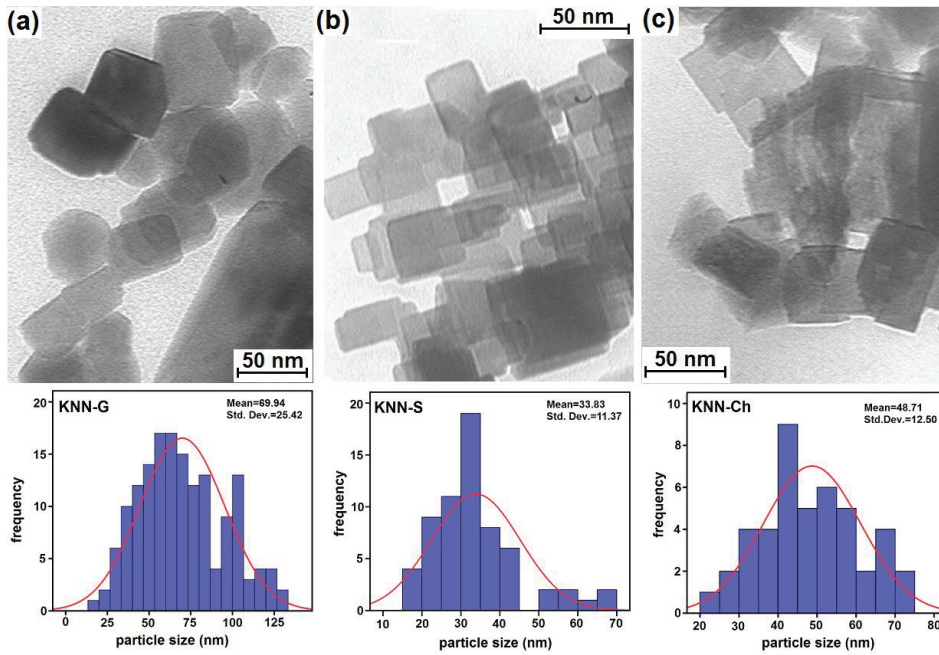

Fig. 5. (Color online) TEM micrographs of (a) KNN-G, (b) KNN-S and (c) KNN-Ch calcined at 600°C in three different media.

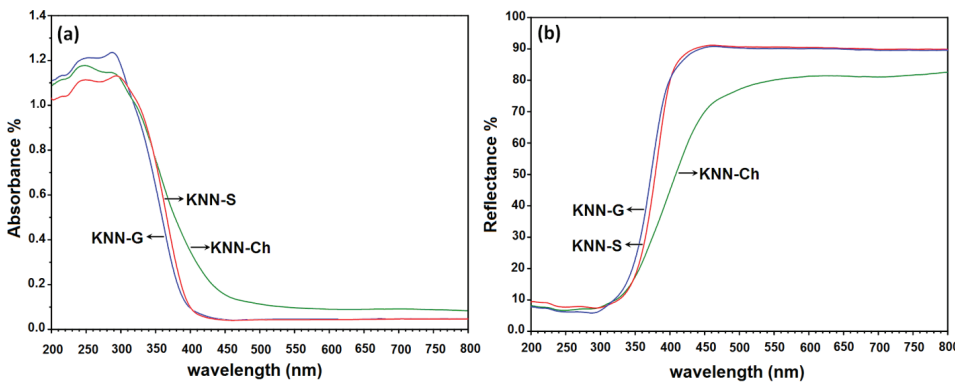

Fig. 6. (Color online) (a) UV-Vis absorbance and (b) reflectance spectra of KNN calcined at 600°C in three different media.

versus $h\nu$ was plotted and E_g estimated from the intersection of the tangent with the x-axis. Study of the density of states (DOS) of $KNbO_3$ and $NaNbO_3$ have shown an indirect band gap for these compounds, in which the energy band gap has been assigned between Nb $4d$ and O $2p$ levels.[23,24] Therefore, the band gaps of our samples were considered to be indirect and the value of m was chosen 2 (Fig. 7). The band gap values of KNN-G, KNN-S and KNN-Ch were then found

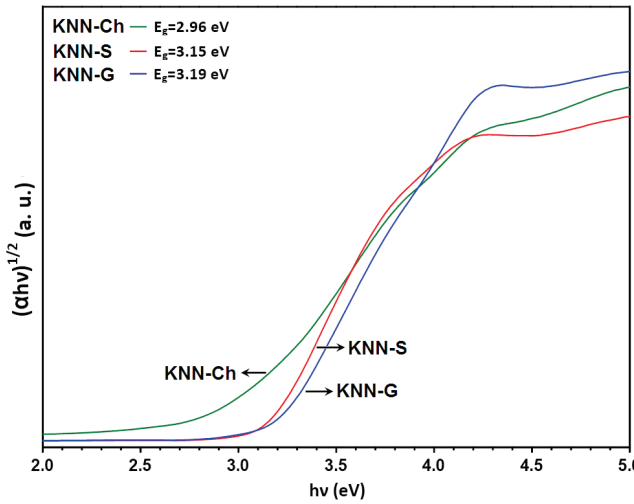

Fig. 7. (Color online) $(\alpha h\nu)^{1/2}$ versus $h\nu$ for the KNN prepared at three different media.

to be 3.19, 3.15 and 2.96 eV, respectively indicating that the energy band gap of KNN-Ch sample is remarkably smaller than the other two.

4. Conclusion

$(K_{0.5}Na_{0.5})NbO_3$ (KNN) nanopowders were synthesized by a facile "green" route using natural polymers: gelatin, starch and chitosan as polymerization agents. The optimum calcination temperature was chosen as 600°C, based on the TGA results. The XRD patterns showed that the prepared powders have orthorhombic phase structures and no remarkable extra peaks were detected. The average size of the crystallites and the lattice strain were calculated using Scherrer formula and SSP method. TEM images showed that the synthesized nanopowders have cubic shape with the average sizes of about 69, 34 and 49 nm for KNN-G, KNN-S and KNN-Ch, respectively. Our results showed that the distribution of KNN nanoparticles prepared in gelatin medium (KNN-G) is more homogenous comparing to KNN-S and KNN-Ch nanoparticles. The average size of KKN-G nanoparticles is bigger than KNN-S and KKN-Ch with better crystallinity and the average size of KNN-S nanoparticles is smaller than KNN-G and KNN-Ch. The optical energy band gap of the prepared samples were estimated from UV-Vis diffused reflectance results using the Kubelka–Munk method and was obtained 3.19, 3.15 and 2.96 eV for KNN-G, KNN-S and KNN-Ch, respectively. So the energy band gap of the sample synthesized using chitosan is remarkably smaller compared to the samples prepared in gelatin and starch media.

Acknowledgments

Authors would like to thank Mrs. R. Pesyan from Central Laboratory of Ferdowsi University of Mashhad for her assistance on TEM imaging.

References

1. P. Kumar, M. Pattanaik and Sonia, *Ceram. Int.* **39** (2013) 65.
2. P. Palei, M. Pattanaik and P. Kumar, *Ceram. Int.* **38** (2012) 851.
3. T. Chen, T. Zhang, J. F. Zhou, J. W. Zhang, Y. H. Liu and G. C. Wang, *Indian J. Phys.* **86**(2012) 443.
4. T. Zhang, K. Zhao, J. Yu, J. Jin, Y. Qi, H. Li, X. Hou and G. Liu, *Nanoscale* **5** (2013) 8375.
5. F. Dutto, C. Raillon, K. Schenk and A. Radenovic, *Nano Lett.* **11** (2011) 2517.
6. H. Shi, X. Li, D. Wang, Y. Yuan, Z. Zou and J. Ye, *Catal. Lett.* **132** (2009) 205.
7. R. Wang, Y. Zhu, Y. Qiu, C. F. Leung, J. He, G. Liu and T. C. Lau, *Chem. Eng. J.* **226** (2013) 123.
8. L. Egerton and D. M. Dillon, *J. Am. Ceram. Soc.* **42** (1959) 438.
9. S. Yamazoe, T. Kawawaki, K. Shibata, K. Kato and T. Wada, *Chem. Mater.* **23** (2011) 4498.
10. T. Maeda, N. Takiguchi, M. Ishikawa, T. Hemsel and T. Morita, *Mater. Lett.* **64** (2010) 125.
11. S. Kim, J. H. Lee, J. Lee, S. W. Kim, M. H. Kim, S. Park, H. Chung, Y. I. Kim and W. Kim, *J. Am. Chem. Soc.* **135** (2013) 6.
12. M. R. Joung, I. T. Seo, J. S. Kim, H. Xu, G. Han, M. G. Kang, C. Y. Kang, S. J. Yoon and S. Nahm, *Acta Mater.* **61** (2013) 3703.
13. L. Li, Y. Q. Gong, L. J. Gong, H. Dong, X. F. Yi and X. J. Zheng, *Mater. Design* **33** (2012) 362.
14. X. Kong, D. Hu, P. Wen, T. Ishii, Y. Tanaka and Q. Feng, *Dalton Trans.* **42** (2013) 7699.
15. D. Q. Zhang, Z. C. Qin, X. Y. Yang, H. B. Zhu and M. S. Cao, *J. Sol–Gel Sci. Technol.* **57** (2011) 31.
16. Y. Cao, K. Zhu, H. Zheng, J. Qiu and H. Gu, *Particuology* **10** (2012) 777.
17. Y. Cao, K. Zhu, J. Qiu, X. Pang and H. Ji, *Solid State Sci.* **14** (2012) 655.
18. S. Wohlrab, M. Weiss, H. Du and S. Kaskel, *Chem. Mater.* **18** (2006) 4227.
19. G. H. Khorrami, A. K. Zak, A. Kompany and R. Yousefi, *Ceram. Int.* **38** (2012) 5683.
20. J. Wu, D. Xiao and J. Zhu, *Recent Patents Mater. Sci.* **2** (2009) 140.
21. E. K. Goharshadi, S. Samiee and P. Nancarrow, *J. Colloid Interf. Sci.* **356** (2011) 473.
22. R. Al Gaashani, S. Radiman, Y. Al Douri, N. Tabet and A. R. Daud, *J. Alloys Compd.* **521** (2012) 71.
23. H. Shi and Z. Zou, *J. Phys. Chem. Solids* **73** (2012) 788.
24. P. Li, S. Ouyang, G. Xi, T. Kako and J. Ye, *J. Phys. Chem. C* **116** (2012) 7621.